António Velez Marques*, Jorge Rencoret, Ana Gutiérrez, José C. del Río and Helena Pereira

Ferulates and lignin structural composition in cork

Abstract: The structure of lignin and suberin, and ferulic acid (FA) content in cork from *Quercus suber* L. were studied. Extractive-free cork (Cork), suberin, desuberized cork ($Cork_{sap}$), and milled-cork lignins (MCL) from Cork and $Cork_{sap}$ were isolated. Suberin composition was determined by GC-MS/FID, whereas the polymers structure in Cork, Corksap, and MCL was studied by Py-TMAH and 2D-HSQC-NMR. Suberin contained 94.4% of aliphatics and 3.2% of phenolics, with 90% of ω-hydroxyacids and α,ω-diacids. FA represented 2.7% of the suberin monomers, overwhelmingly esterified to the cork matrix. Py-TMAH revealed significant FA amounts in all samples, with about 3% and 6% in cork and cork lignins, respectively. Py-TMAH and 2D-HSQC-NMR demonstrated that cork lignin is a G-lignin (>96% G units), with a structure dominated by β–*O*–4′ alkyl-aryl ether linkages (80% and 77% of all linkages in MCL and MCL_{sap}, respectively), followed by phenylcoumarans (18% and 20% in MCL and MCL_{sap}, respectively), and smaller amounts of resinols (ca. 2%) and dibenzodioxocins (1%). HSQC also revealed that cork lignin is heavily acylated (ca. 50%) exclusively at the side-chain γ-position. Ferulates possibly have an important function in the chemical assembly of cork cell walls with a cross-linking role between suberin, lignin and carbohydrates.

Keywords: 2D-NMR, ferulic acid, HSQC, Py-TMAH, *Quercus suber*, suberin

***Corresponding author: António Velez Marques,** Instituto Superior de Engenharia de Lisboa, Rua Conselheiro Emídio Navarro 1, 1959-007 Lisboa, Portugal, Phone: +351 218317172, Fax: +351 218317267, e-mail: avelez@deq.isel.ipl.pt

Jorge Rencoret, Ana Gutiérrez and José C. del Río: Instituto de Recursos Naturales y Agrobiología de Sevilla, CSIC, P.O. Box 1052, 41080 Sevilla, Spain

Helena Pereira: Centro de Estudos Florestais, Instituto Superior de Agronomia, Universidade de Lisboa, Tapada da Ajuda, 1349-017 Lisboa, Portugal. http://orcid.org/0000-0002-5393-4443

DOI 10.1515/hf-2015-0014
Received January 12, 2015; accepted April 21, 2015; previously published online May 22, 2015

Introduction

Cork is a cellular tissue with a protective function that is present in the outer barks of higher plants, as part of the periderm and the rhytidome, in variable proportion in different species. A paradigmatic and well-known example is the cork from *Quercus suber* L., the cork oak, which is commercially exploited as a valuable raw material, and quite intensively studied for that reason (as reviewed by Pereira 2007). Cork is also present in the periderm of other plant parts, such as in potato (*Solanum tuberosum* L.) tuber.

The chemical composition of cork is characterized by suberin as the main structural component of the cell wall (CW) (Pereira 2013). Suberin is considered by most researchers as the aliphatic macromolecular structural component of cork CWs, which is topochemically linked to lignin as the structural phenolic polymer of the CW (Marques et al. 1999; Pereira 2007). The composition of the aliphatic monomers and inter-monomeric linkages in suberin are now fairly well established: suberin is a polyester network composed of glycerol and long-chain poly-functional fatty acids, ω-hydroxyacids, and α,ω-diacids (Graça and Pereira 1997, 2000a; Bento et al. 1998, 2001; Olivella and del Río 2011). This composition has been validated in corks from barks of other species, e.g., *Q. variabilis* Blume (Miranda et al. 2013), *Q. cerris* L. (Şen et al. 2010), *Pseudotsuga menziesii* (Mirb.) Franco (Graça and Pereira 2000b), and *Betula pendula* Roth. (Pinto et al. 2009).

However, the supramolecular architecture of suberin and the assembly of the cork CW components are still not fully understood, particularly regarding the differentiation between lignin and the suberin-associated polyphenolic moiety. The presence of lignin in corks from tree barks has been demonstrated, and it has been found to be composed mostly of guaiacyl (G) lignin, with only minor amounts of syringyl (S) and *p*-hydroxyphenyl (H) units (Marques et al. 1996, 1999, 2006; Marques and Pereira 2013). However, the structure of the phenolic network

involved in suberization is still a matter of discussion, and particularly when addressing cork tissues in plants other than tree barks (Kolattukudy 2001; Bernards 2002). Lignin with an S-G-core has been identified in potato suberized tissues by thioacidolysis (Lapierre et al. 1996), cinnamyl alcohol precursors were identified by ^{13}C-NMR (Yan and Stark 2000), and a lignin-like polyphenolic domain built up by hydroxycinnamic acid precursors was identified by ^{13}C-NMR studies (Bernards et al. 1995).

The inclusion of a polyphenolic network in the suberin matrix and its relationship with the other CW polymers are still unclear. The occurrence of ferulates in suberized CWs is well known, although the amounts found in suberin extracts largely depend on the depolymerization procedures – which is <1% in suberin saponification products – that only cleaves ester bonds (Graça and Pereira 1998, 2000a,b), or amounts up to 9% in more aggressive tetramethylammonium hydroxide thermochemolysis (Py-TMAH), which cleaves both ester and ether bonds (García-Vallejo et al. 1997; Bento et al. 2001; Olivella and del Río 2011).

Lignin is a complex heterogeneous polymer built-up by an oxidative coupling of the three main *p*-hydroxycinnamyl alcohol monolignols (*p*-coumaryl, coniferyl, and sinapyl alcohols). Moreover, other precursors may also be involved in the monolignol biosynthetic pathway, such as ferulates (Sederoff et al. 1999; Bonawitz and Chapple 2010; Ralph 2010). Ferulates participate in cross-linking between cell-wall polymers (Hatfield et al. 1999; Ralph et al. 2004a; Ralph 2010). Ferulic acid (FA) can be esterified or etherified with the lignin bulk depending on its role in the free-radical mechanism, which can be a simple quinone methide trapping (Scalbert et al. 1986) and/or direct coupling within the free-radical polymerization chain, from which FA cannot be easily released (del Río et al. 2007a; Ralph 2010). The presence of ferulates in lignins can be easily underestimated and biased by conventional analytical pyrolysis techniques because of decarboxylation reactions (Martín et al. 1995; del Río et al. 2007a).

The biosynthetic pathway leading to the supramolecular assembly of the different chemical domains in cork CWs is far from being understood. Most biochemical studies were oriented on the biosynthesis of the suberin aliphatic polymer. Previous research focused on suberin from *Arabidopsis* and potato species and on the identification of genes and enzymes that influence cork phellem development and suberin aliphatics and ferulate biosynthesis (Soler et al. 2007; Gou et al. 2009; Molina et al. 2009; Serra et al. 2009, 2010a,b; Boher et al. 2013). The polymeric aromatic domain associated with the aliphatic suberin in the cork CW, usually described as a lignin-like or aromatic-suberin, is not well investigated. Evidence for an independent biosynthetic pathway involving the aromatics is given by Serra et al. (2009), and experimental results exist for the involvement of H_2O_2 (needed in lignin biosynthesis) in suberization (Soler et al. 2007).

Research on the biosynthetic pathway of lignin is better developed (Ralph et al. 2004b; Bonawitz and Chapple 2010; Vanholme et al. 2010) but not free from controversies. There are indications that metabolic variations in the supply of lignin precursors may increase the incorporation of minor components, such as ferulates (Sederoff et al. 1999). Concerning the suberized tissues, there is a hypothesis that ferulates play a cross-linking role in the molecular assembly in the cork CWs, which are probably also a part of the lignin moiety as already seen in corks from tree barks (Santos and Graça 2006; Gou et al. 2009).

The aim of the present study was to look more closely at the role of ferulates in the macromolecular structural assembly of cork CWs, in which suberin and lignin structures are associated. It was demonstrated that a part of ferulates can be extracted from the CW (Kumar and Pruthi 2014), but no attempt was made to study the solvent-extractable non-structural ferulates. Various aspects of ferulates in extractive-free cork, desuberized cork, and in other cork polymers were addressed by analytical pyrolysis in the presence of tetramethylammonium hydroxide as methylating reagent (Py-TMAH) and two-dimensional nuclear magnetic resonance spectroscopy (2D-NMR).

Materials and methods

Cork from cork oak (*Q. suber* L.) was obtained as industrial cork powder (particle size <80 mesh) from a cork mill in Portugal. Cork was oven-dried and exhaustively extracted in a Soxhlet apparatus with a solvent sequence of dichloromethane, ethanol, and water, and then dried in an oven at 60°C and in vacuum over P_2O_5. The total content of extractives amounted to 21%, but no attempt was made to analyze this fraction in the present work. Different fractions were isolated from cork, as detailed in Figure 1. Milled-cork lignin (MCL) was isolated directly from cork as previously described (Marques et al. 1994). MCL from desuberized cork (MCL_{sap}) was isolated as previously described (Marques et al. 1996).

Depolymerization and analysis of suberin

The suberin content of cork was determined by transesterification with sodium methoxide in dry methanol (0.5% w/v) (Graça and Pereira 2000b). Suberin depolymerization was made under reflux for 4 h. The reaction products were filtered, washed with fresh methanol, and the pH of the extracts was adjusted to 6 with 0.5 M H_2SO_4 in

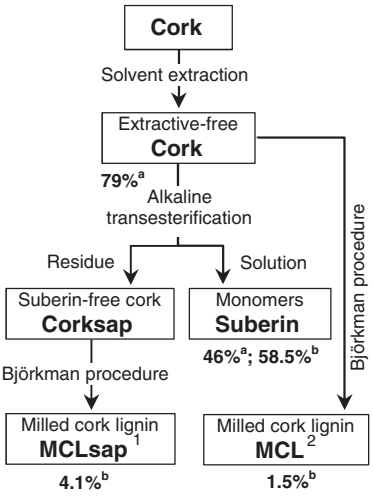

Figure 1: Preparation and isolation scheme for the *Quercus suber* cork samples. 1) MCL_{sap} isolation described in Marques et al. (1996). 2) MCL isolation described in Marques et al. (1994).
[a]Cork basis, [b]extractive-free cork basis.

methanol. The residual solid was dried and weighed. Suberin was determined gravimetrically from the solid mass loss after depolymerization. The suberin content of cork was determined as the solid mass loss. This approach is reliable and assures that the real *in situ* mass is measured and that all the solubilized monomers from the polyester matrix are taken into account including glycerol. The methanolic extract was evaporated to dryness and suspended in water. The suberin depolymerizates were recovered by extraction with dichloromethane. Total polyester depolymerization was confirmed by the ester band at 1740 cm^{-1} in the FTIR spectra of the dried residual depolymerized cork, i.e., desuberized cork ($Cork_{sap}$).

Trimethylsilyl (TMS) derivatives from the suberin extract were prepared by reaction with a 1:1 (v/v) mixture of pyridine and N,O-bis(trimethylsilyl)trifluoroacetamide (BSTFA with 1% trimethylchlorosilane). The derivatized extract was analyzed by GC-MS/FID with a Thermo Trace Ultra Polaris Ion Trap apparatus from Thermo Finnigan (Austin, TX) equipped with a fused-silica capillary column ZB-5HT (30 m×0.25 mm×0.10 μm) from Phenomenex. Identification and quantification were performed separately by GC-MS and GC-FID analysis, respectively. Individual peak areas of the chromatogram were determined by automatic integration (Thermo Excalibur software 1.4 SR1), with manual corrections when necessary. The identification of the compounds was made by comparison of retention times (RTs) and mass spectra with those from our own collection of authentic standards and by comparison with mass spectral libraries (NIST/EPA/NIH). Quantitation of the identified compounds was determined by the relative peak areas related to the total area.

Py-TMAH analysis

Pyrolysis (Py) coupled with gas chromatography/mass spectrometry (Py-GC/MS) of cork and milled-cork lignins (MCLs) was performed using EGA/PY-3030D micro-furnace pyrolyzer (Frontier Laboratories Ltd., Fukushima, Japan) connected to an Agilent 7820A GC (Agilent Technologies, Inc., Santa Clara, CA, USA) equipped with a DB-1701 fused-silica capillary column (60 m×0.25 mm i.d., 0.25 μm film thickness) and an Agilent 5975 mass selective detector (EI at 70 eV) in the presence of tetramethylammonium hydroxide (TMAH). Approximately 0.1 mg of sample was mixed with 1 μL of TMAH (25%, w/w, methanol solution) before pyrolysis. The Py temperature was set at 500°C. The oven temperature was heated from 45°C (4 min) to 280°C (10 min) at 4°C min^{-1}. He was chosen as the carrier gas (2 ml min^{-1}). The compounds were identified based on the Wiley (John Wiley and Sons, Hoboken, NJ, USA) and NIST/EPA/NIH 2011 (National Institute of Standards and Technology, Gaithersburg, MD, USA) mass spectral libraries and with those from our own collection of standards. Peak molar areas were calculated for the suberin and lignin-degradation products, the summed areas were normalized and expressed as percentages.

2D-HSQC-NMR

For NMR analysis of cork and MCLs, about 40 mg of sample was dissolved in 0.75 ml of deuterated dimethylsulfoxide (DMSO-d_6). 2D-NMR HSQC spectra were acquired at 25°C on a Bruker AVANCE III 500 MHz spectrometer (Bruker, Karlsruhe, Germany) fitted with a cryogenically cooled 5 mm TCI gradient probe with inverse geometry (proton coils closest to the sample). The 2D ^{13}C–^{1}H correlation spectra were performed with an adiabatic HSQC pulse program (Bruker standard pulse sequence "hsqcetgpsisp2.2") and the following parameters: spectra were acquired from 10 to 0 ppm in F2 (^{1}H) with 1000 data points for an acquisition time of 140 ms, an interscan delay of 1 s, and from 165 to 0 ppm in F1 (^{13}C) with 256 increments of 32 scan, for a total acquisition time of 2 h 40 min. The $^{1}J_{CH}$ was 145 Hz. Processing used typical matched Gaussian apodization in ^{1}H and a squared cosine bell in ^{13}C. The central solvent peak served as an internal reference (δ_C/δ_H 39.5/2.49). 2D-NMR cross-signals were assigned as in previous studies (Ralph et al. 2004c; Rencoret et al. 2008, 2009, 2011; del Río et al. 2011, 2012). Integration of the lignin and FA cross-signals were performed separately for the different regions of the HSQC spectra, which contain signals that correspond to chemically analogous carbon-proton pairs. For these signals, the $^{1}J_{CH}$ coupling value is similar and the semiquantitative estimation of the relative abundance of the different substructures is based on the peak integrals. In the aliphatic-oxygenated region (δ_C/δ_H 50–90/2.5–5.8), the relative abundances of side-chains involved in inter-unit linkages were estimated from the C_α–H_α correlations to avoid possible interference from homonuclear ^{1}H–^{1}H couplings. In the aromatic/unsaturated region (δ_C/δ_H 100–155/6.0–8.0), the $S_{2,6}$, G_2, $H_{2,6}$ and FA_2 signals served as the bases for estimating the relative abundances of the different lignin and FA units.

Results and discussion

As shown in Figure 1, different fractions, including the extractive-free cork (Cork), the suberin monomers and the solid residue obtained after suberin removal by depolymerization ($Cork_{sap}$), and the MCLs isolated from Cork (MCL) and from $Cork_{sap}$ (MCLsap), were isolated from cork and analyzed. The presence of FA in all these samples was analyzed. The suberin monomers obtained after depolymerization were analyzed by GC-MS/FID. Under the reactive

conditions applied, all the monomeric units with ester links in the polymers were released. The polymeric fractions of the Cork, $Cork_{sap}$, MCL, and MCL_{sap} samples were analyzed by Py-TMAH and 2D-HSQC-NMR.

Suberin analysis

The suberin content of the cork was 58.5% based on o.d. Cork (46.0% on an o.d. cork without extraction). This value is within the variability of cork composition, although it is higher than the reported mean of 51.1% (of extractive-free cork) (Pereira 2013). The desuberized cork residue ($Cork_{sap}$) did not show the carbonyl ester band at 1740 cm^{-1} (results not shown), and thus it was concluded that all ester bonds of the suberin skeleton were broken and that all the components that were previously ester-linked in the cork matrix were released.

Table 1 presents the monomeric composition of the cork suberin recovered after depolymerization and dichloromethane extraction. With the analytical procedures applied, all the released OH groups were analyzed as trimethylsilyl ethers and the *in situ* esterified -COOH groups as methyl esters, whereas the *in-situ* free -COOH groups were derivatized to trimethylsilyl esters and identified as such. Small amounts of the ester derivatives of hydroxy acids and diacids were identified with one trimethylsilyl ester group (TMS). Their origin can be a terminal monomer with one *in situ* free acid group or the result of some hydrolysis during neutralization of the suberin extract. For simplicity,

Table 1: Composition of suberin extract from *Quercus suber* cork as obtained by GC-FID.

Compound	%	Compound	%
Glycerol	**0.01**	1-Alkanols	**1.77**
Phenolics	**2.92**	Octadecanol	0.03
Ferulic acid (total)	**2.71**	Eicosanol	0.20
Vanillin	0.09	Docosanol	0.65
4-Hydroxy-3-methoxy-benzoic acid	0.04	Tetracosanol	0.70
2-(4-hydroxy-3-methoxyphenyl)-acetic acid	tr.	Hexacosanol	0.19
3,4-Dihydroxybenzoic acid	0.01	Monoacids	**1.58**
Coumaric acid	0.01	9-Oxo-nonanoic acid	0.04
cis-Ferulic acid	0.05	Hexadecanoic acid	0.07
trans-Ferulic acid	2.66	Linoleic acid	0.03
4-Hydroxy-3-methoxycinnamaldehyde	0.02	Oleic acid	0.14
3,4-Dihydroxycinnamic acid	0.04	Stearic acid	0.04
ω-Hydroxyacids	**52.89**	Eicosanoic acid	0.05
ω-Hydroxyacids, saturated	**20.06**	Docosanoic acid	0.79
8-Hydroxyoctanoic acid	0.03	Tetracosanoic acid	0.43
9-Hydroxynonanoic acid	0.05	α,ω-Diacids	**29.48**
14-Hydroxytetradecanoic acid	0.01	α,ω-Diacids, saturated	**6.12**
16-Hydroxyhexadecanoic acid	1.00	Hepta-1,7-dioic acid	0.01
18-Hydroxyoctadecanoic acid	0.12	Octan-1,8-dioic acid (Suberic acid)	0.09
20-Hydroxyeicosanoic acid	1.04	Nonan-1,9-dioic acid (Azelaic acid)	0.21
22-Hydroxydocosanoic acid	15.04	Decan-1,10-dioic acid (Sebacic acid)	0.00
23-Hydroxytricosanoic acid	0.08	Undecan-1,11-dioic acid	0.01
24-Hydroxytetracosanoic acid	2.59	Hexadecan-1,16-dioic acid	1.73
26-Hydroxyhexacosanoic acid	0.10	Eicosan-1,20-dioic acid	0.64
ω-Hydroxyacids, mid-chain substituted	**32.83**	Docosan-1,22-dioic acid	3.43
18-Hydroxyoctadec-9-enoic acid	14.60	α,ω-Diacids, mid-chain substituted	**23.37**
9-Epoxy-18-hydroxy-octadecanoic acid	10.33	Octadec-9-en-1,18-dioic acid	5.10
9,10,18-Trihydroxyoctadecanoic acid	5.14	9-Epoxyoctadecan-1,18-dioic acid	10.44
9-hydroxy acid isomers	2.12	9-Oxooctadecan-1,18-dioic acid	0.26
22-Hydroxydocosenoic acid	0.65	9,10-Dihydroxyoctadecan-1,18-dioic acid	6.83
Triterpenoids	**2.20**	9-Epoxyeicosan-1,20-dioic acid	0.24
Monoacylglycerols	**0.35**	Docosendioic acid	0.24
Unidentified	**8.80**	9,10-Dihydroxyeicosan-1,20-dioic acid	0.24

Results are presented in area percentage relative to total chromatogram area. Values in bold represent partial totals for the suberinic acid functional group class.
tr., Trace amounts.

suberin components are reported in Table 1 in their acid form. Suberin composition is within the expected range for a *Q. suber* cork, with ω-hydroxyacids and α,ω-diacids as the main components and corresponding to 90% of the total amount (Graça and Pereira 2000b; Olivella and del Río 2011). Aliphatics and phenolics represent 94.4% and 3.2% of the identified components, respectively (Table 1).

FA represents 2.7% of the total suberin monomers and 93% of the phenolics. The major part of FA (99%) was identified as the methyl ester derivative of ferulates linked to the suberin matrix. The remaining 1% was identified as a trimethylsilyl ester either derived from an FA that was linked to the cork matrix merely by its phenol group or by hydrolysis of the FA methyl ester. These results are in accordance with previously published studies, which reported that the alkali-releasable FA is mainly bound to the suberin matrix as ferulates (Graça and Pereira 1998; Graça 2010).

The total amount of FA present in the depolymerized suberin is in accordance with the low values found previously (1.0%) and ferulates (0.4%) based on the same procedures (Graça and Pereira 1998, 2000b). However, these data are substantially lower than the 9% FA found with a Py-TMAH procedure (García-Vallejo et al. 1997). As shown below, Py-TMAH also yields 9.3% FA content. This result indicates that a substantial part of FA is bound through alkali-resistant bonds (i.e., ether linkages) that are not cleaved during hydrolysis. However, some ether bond cleavage from lignin cannot be totally neglected as this was found to occur in non-woody biomass under soft alkaline pulping conditions (Iglesias et al. 1996). Small amounts of other phenolic compounds were identified, with vanillin as the second most abundant compound (representing 0.09% of the total suberin monomers). All the identified phenolics are typical lignin products (Ralph et al. 2004a; del Río et al. 2007a).

Py-TMAH

Conventional analytical pyrolysis (Py) is an established analytical tool for compositional analysis of lignocellulosics, and it is particularly valuable for the analysis of lignin moiety. For example, the lignin composition in corks and in their isolated milled lignins (MCLs) was analyzed by Py (Marques et al. 1996, 2006; Marques and Pereira 2013). However, suberin and lignin have a different thermal resistance/behavior and thus their simultaneous analysis by Py is difficult (Marques and Pereira 2013): high temperatures are required by suberin for complete pyrolysis; and alkenes and alkadienes are produced by decarboxylation from the aliphatic polyester matrix (Marques and Pereira 2014), whereas ferulates decarboxylate and less specific compounds, such as 4-vinylguaiacol, which can also arise from the lignin core structure (del Río et al. 1996, 2012), are produced.

Pyrolysis in the presence of tetramethylammonium hydroxide (Py-TMAH) as a methylating reagent helps diminish structural degradation. One speaks about a thermally assisted hydrolysis and methylation (de Leeuw and Baas 1993; del Río et al. 1996), and its advantages are obvious in the case of a complex cork with high amounts of fatty acid and ester functionalities. By this approach, determination of the aliphatic fatty acids of suberin and identification of FA as a relevant component are possible (Bento et al. 1998, 2001; Olivella and del Río 2011).

The Py-TMAH pyrograms of Cork, desuberized cork ($Cork_{sap}$), MCL, and MCL_{sap} are presented in Figure 2. The assignments and the relative molar abundances of the Py degradation products are listed in Table 2. The main compounds identified in the pyrograms correspond to suberinic acids (as their methyl esters) derived from the suberin polymer and to phenolic compounds (as their methyl derivatives) arising from the lignin polymer, as well as from ferulates. Minor amounts of carbohydrate-derived compounds are observable, but these were not identified and quantified.

The profiles of the lignin-derived Py-TMAH products are very similar in the four samples in question. There is a high predominance of guaiacyl-derived products (G products) among the released compounds, namely, 1,2-dimethoxybenzene (2), 3,4-dimethoxytoluene (4), 3,4-dimethoxyphenylethylene (10), 1,2-dimethoxy-4-propenylbenzene (14), 3,4-dimethoxybenzaldehyde (15), 3,4-dimethoxybenzoic acid methyl ester (16), and 3,4-dimethoxyacetophenone (17), among others, including the occurrence of the *threo/erythro* 1-(3,4-dimethoxyphenyl)-1,2,3-trimethoxypropane (26, 27) as the direct Py-TMAH derivative from guaiacylglycerol-β-aryl ether lignin sub-units. This result confirms the known G-rich lignin composition of cork (Marques et al. 1996, 1999, 2006; Marques and Pereira 2013). Minor amounts of H-lignin fragments (without OMe groups), including 4-methoxyphenylethylene (1), 4-methoxybenzaldehyde (5), 4-methoxyacetophenone (8) and 4-methoxybenzoic acid methyl ester (9), were also found. Some S-lignin derived compounds, such as 1,2,3-trimethoxybenzene (7) and 3,4,5-trimethoxybenzoic acid methyl ester (24), could also be observed. However, the fact that 3,4,5-trimethoxybenzoic acid methyl ester (24) was found in high amounts in $Cork_{sap}$ and only in minor amounts in the respective MCL_{sap} sample indicates that this compound may arise from non-lignin moieties, most probably from gallic and/or ellagic acids, that give rise to the same compound upon Py-TMAH. This interpretation is also supported by the absence of other S-lignin fragment in these

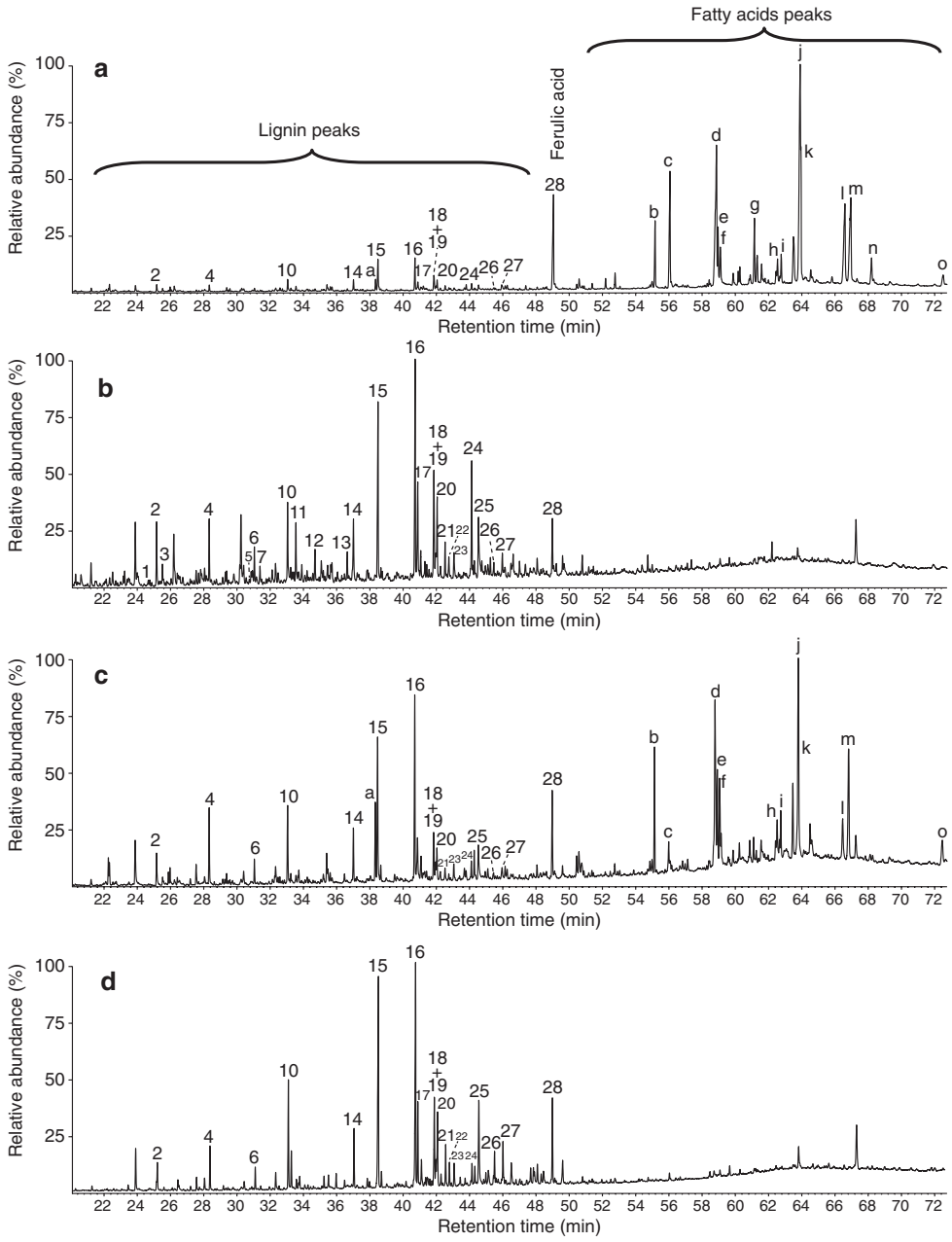

Figure 2: Py/TMAH-GC/MS chromatograms of *Quercus suber* cork and milled-cork lignin samples. (a) Extracted cork (Cork); (b) $Cork_{sap}$; (c) MCL; (d) MCL_{sap}. The assignments and relative abundances of the released compounds are listed in Table 2.

samples. Therefore, the relative abundance of S-lignin in the $Cork_{sap}$ may be highly overestimated upon Py-TMAH by the occurrence of gallic and/or ellagic acids. Other related compounds, such as 1,2,4-trimethoxybenzene (11), 1,3,5-trimethoxybenzene (12) and 2,4,6-trimethoxytoluene (13), were also released not from lignin but from other polymers, including carbohydrates (del Río et al. 1998).

FA was detected in all samples in significant amounts, accounting for 9.3% in Cork, 3.3% in $Cork_{sap}$, 4.5% MCL, and 5.4% in MCL_{sap}. This finding indicates that FA plays a structural role in the supramolecular assembly of the cork CW, as previously discussed (Graça and Pereira 1998). In the depolymerized suberin extract (obtained by transesterification), the FA content was 2.7% (Table 1), whereas in the remaining solid residue, $Cork_{sap}$, FA accounted for 3.3% (Py-TMAH, Table 2). $Cork_{sap}$ represented 41.5% of the Cork, and this means that the FA in cork should be about 3% (0.585*2.7+0.415*3.3). This value is not in agreement with the high FA content (9%) determined in Cork by Py-TMAH (Table 2). This value can be explained by the biased Py-TMAH results with an underestimation of the carbohydrates in cork. In fact, in this pyrogram,

Table 2: Lignin-derived and related compounds and fatty acids (as their methyl derivatives) released upon Py-GC/MS in the presence of TMAH of *Quercus suber* cork and derived samples.

Peak	Compound	Cork	$Cork_{sap}$	MCL	MCL_{sap}
	Lignin-derived (and related) compounds				
1	4-Methoxyphenylethylene	0.04	0.63	0.11	0.06
2	1,2-Dimethoxybenzene	0.86	4.78	2.87	2.66
3	1,4-Dimethoxybenzene	0.29	1.56	0.55	0.08
4	3,4-Dimethoxytoluene	0.65	4.33	5.03	3.70
5	4-Methoxybenzaldehyde	0.05	0.50	0.19	0.15
6	4-Ethyl-1,2-dimethoxybenzene	0.28	2.09	1.42	1.69
7	1,2,3-Trimethoxybenzene	0.15	1.26	0.21	0.32
8	4-Methoxyacetophenone	0.05	0.37	0.15	0.00
9	4-Methoxybenzoic acid methyl ester	0.27	1.38	0.46	0.00
10	3,4-Dimethoxyphenylethylene	1.19	5.45	5.36	9.23
11	1,2,4-Trimethoxybenzene	0.46	3.81	0.43	0.81
12	1,3,5-Trimethoxybenzene	0.17	2.23	0.12	0.03
13	2,4,6- Trimethoxytoluene	0.17	1.84	0.04	0.00
14	1,2-Dimethoxy-4-propenylbenzene	0.87	4.69	3.13	4.31
15	3,4-Dimethoxybenzaldehyde	3.13	13.68	10.12	21.59
16	3,4-Dimethoxybenzoic acid methyl ester	2.49	13.26	9.82	18.42
17	3,4-Dimethoxyacetophenone	0.60	6.83	3.33	6.23
18	*cis*-1-(3,4-dimethoxyphenyl)-2-methoxyethylene	0.79	4.55	1.94	3.44
19	3,4-Dimethoxyphenylacetic acid methyl ester	0.70	2.78	0.93	3.39
20	*trans*-1-(3,4-dimethoxyphenyl)-2-methoxyethylene	0.68	4.16	1.70	5.23
21	*E*-1-(3,4-dimethoxyphenyl)-1-methoxyprop-1-ene	0.35	1.86	0.69	2.63
22	*Z*-1-(3,4-dimethoxyphenyl)-1-methoxyprop-1-ene	0.16	1.17	0.25	1.52
23	1-(3,4-dimethoxyphenyl)-1-propanone	0.17	1.70	0.96	1.86
24	3,4,5-Trimethoxybenzoic acid methyl ester	0.40	5.63	0.76	1.32
25	*trans*-1-(3,4-dimethoxyphenyl)-3-methoxyprop-1-ene	0.41	4.58	2.57	2.37
26	*threo/erythro* 1-(3,4-dimethoxyphenyl)-1,2,3-trimethoxypropane	0.12	0.66	0.33	1.60
27	*threo/erythro* 1-(3,4-dimethoxyphenyl)-1,2,3-trimethoxypropane	0.17	0.98	0.47	1.98
28	*trans*-3-(3,4-dimethoxyphenyl)-propenoic acid methyl ester	9.32	3.25	4.45	5.40
	% H	2.9	3.3	1.7	0.2
	% G	93.3	88.8	96.4	98.0
	% S	3.8	7.9	1.9	1.8
	Suberin-derived fatty acids				
a	Nonanedioic acid, dimethyl ester	0.79	nd	3.97	nd
b	Hexadecanedioic acid, dimethyl ester	3.78	nd	4.37	nd
c	ω-Methoxyoleic acid, methyl ester	7.69	nd	1.05	nd
d	9-Octadecenedioic acid, dimethyl ester	14.30	nd	8.41	nd
e	Docosanoic acid, methyl ester	2.66	nd	3.03	nd
f	Octadecanedioic acid, dimethyl ester	0.91	nd	0.62	nd
g	9,10-Epoxyoctadecanoic acid, methyl ester	3.87	nd	0.87	nd
h	Tetracosanoic acid, methyl ester	1.04	nd	1.15	nd
i	Eicosanedioic, dimethyl ester	1.16	nd	1.29	nd
j	ω-Methoxydocosanoic acid, methyl ester	17.69	nd	7.49	nd
k	9-10-Dimethoxyoctadecanodioic acid, dimethyl ester	3.58	nd	1.90	nd
l	9,10,18-Trimethoxyoctadecanoic acid, methyl ester	7.23	nd	0.95	nd
m	Docosanedioic acid, dimethyl ester	7.79	nd	5.12	nd
n	ω-Methoxytetracosanoic acid, methyl ester	1.63	nd	0.00	nd
o	Tetracosanedioic acid, dimethyl ester	0.88	nd	1.39	nd
	Total phenolics	25.01	100.00	58.40	100.00
	Ferulic acid	9.32	3.25	4.45	5.40
	Monoacids	7.57	nd	5.99	nd
	α,ω-Diacids	33.20	nd	27.07	nd
	ω-Hydroxyacids	34.23	nd	8.54	nd

Results are presented in molar area percentage relative to total area of identified compounds.
nd, not detected.

aliphatics represented almost 75% and phenolics a total of 25%, but no carbohydrate-derivatives were identified. Therefore, the Py-TMAH results of this sample overestimated the content of aliphatics and should be corrected by considering the known cork polysaccharide content of 20% (Pereira 2013). The occurrence of carbohydrates can be easily observed in the 2D-HSQC-NMR (as shown below) but are hardly detectable by Py-TMAH as a consequence of the high Py temperatures. With this correction, the content of aliphatics, phenolics, and FA should be approximately 60%, 20%, and 7%, respectively, and this estimation is in accordance with the determined suberin and lignin content of 58.5% of cork (Pereira 2013).

However, this corrected value for the FA content (7%) still seems to be overestimated. This may indicate that FA may also be ether-linked to the polymeric matrix, which cannot be cleaved by transesterification but are released upon Py-TMAH. Transesterification only cleaves ester bonds (and thus makes FA esterified units detectable), whereas Py-TMAH cleaves both ester and ether bonds and releases the total FA molecules linked to the polymer matrix. The differences between ether and ester bonds lability in the alkaline medium can therefore be associated with the overrating of FA by Py-TMAH in cork. If cork lignin was analysed, FA overrating would not have occurred.

$Cork_{sap}$ should be composed approximately of 50% lignin and 50% carbohydrates owing to the chemical composition of cork (Pereira 2013). The FA in $Cork_{sap}$ accounted for 3.3%, and thus the FA content in $Cork_{sap}$ lignin should be about 6.6% (given that carbohydrates do not include FA). The FA content determined in MCL_{sap} was slightly lower at 5.4% but in perfect accordance considering that some FA involved in cross-links could be lost to lignin-carbohydrate complexes upon the MCL_{sap} isolation (Marques et al. 1996).

The H/G/S ratios determined by Py-TMAH are in accordance with previously reported data (Marques et al. 1996, 2006; Marques and Pereira 2013) and confirm that cork lignin is mainly a G-lignin, in which FA is partially incorporated. The H/G/S ratios determined by conventional pyrolysis (1/98/1–2) for MCL_{sap} (Marques et al. 1996) do not seem to be affected by the inclusion of 4-vinylguaiacol arising from decarboxylation of FA (del Río et al. 2007a), as previously predicted (Marques and Pereira 2013).

Some differences were observed in the suberinic fatty acids profile obtained by Py-TMAH of cork (Table 2) in comparison with the reference results obtained by the GC analysis of the depolymerized suberin extract (Table 1). Upon Py-TMAH, saturated acids (monoacids and diacids) were overestimated (17.2% vs. 7.5%), unsaturated ω-hydroxyacids were underestimated (7.7% vs. 15.3%), and 9,10-epoxides of ω-hydroxyacids and diacids were not detected, although their content in the GC analysis of suberin was 21%. The same kind of ambiguities were observed in other Py-TMAH analyses of cork (Bento et al. 1998; del Río and Hatcher 1998), where the conversion of 9,10-epoxyacids to 9,10-dihydroxyacids and other unidentified derivatives biased the occurrence of epoxides by reaction of the epoxide ring with TMAH.

Aliphatic acids were observed in the Py-TMAH of MCL but were absent in the MCL_{sap} sample (Table 2). This result means that suberinic acids are exclusively linked by alkaline-labile bonds to the lignin core and not by alkaline-resistant ether bonds. However, $KMnO_4$ oxidation of these same cork lignins (Marques et al. 1999) indicate the presence in MCL_{sap} of residual amounts of suberinic acids, which leads to the assumption that alkaline-resistant covalent links are involved (although to a very low extent) in the lignin-suberin core matrices of cork CWs. These findings seem closely related with reports that identified an alkaline-resistant aliphatic polymer, named suberan, in suberized tissues (Tegelaar et al. 1995; Turner et al. 2013).

2D-HSQC-NMR

The 2D-HSQC-NMR spectra of *Q. suber* cork (Cork and $Cork_{sap}$) and MCL and MCL_{sap} are presented in Figure 3. The main lignin correlation peaks assigned in the HSQC spectra are listed in Table 3, and the main substructures are depicted in Figure 4. The main types of structural moieties include aliphatic chains from suberin aliphatic acids, lignin, and carbohydrates. In general terms, the analyses by 2D-HSQC-NMR are in close agreement with those of Py-TMAH, except for the occurrence of carbohydrates that were biased upon Py-TMAH. Accordingly, Cork is composed mostly of aliphatic acids, and carbohydrates and smaller amounts of lignin moieties and ferulates are present. $Cork_{sap}$ contains carbohydrates and lignin and small amounts of ferulates, but is depleted in aliphatic acids because of alkaline transesterification, in agreement with the Py-TMAH results (Figure 1). The MCL is enriched in lignin moieties but still contains some associated aliphatic acids and carbohydrates, whereas the MCL_{sap} is highly enriched in lignin moieties and depleted in carbohydrates and aliphatic acids, as already observed by Py-TMAH.

The side-chain region of the spectra gave useful information about the different inter-unit linkages present in the lignin moieties. In this region, cross-signals from

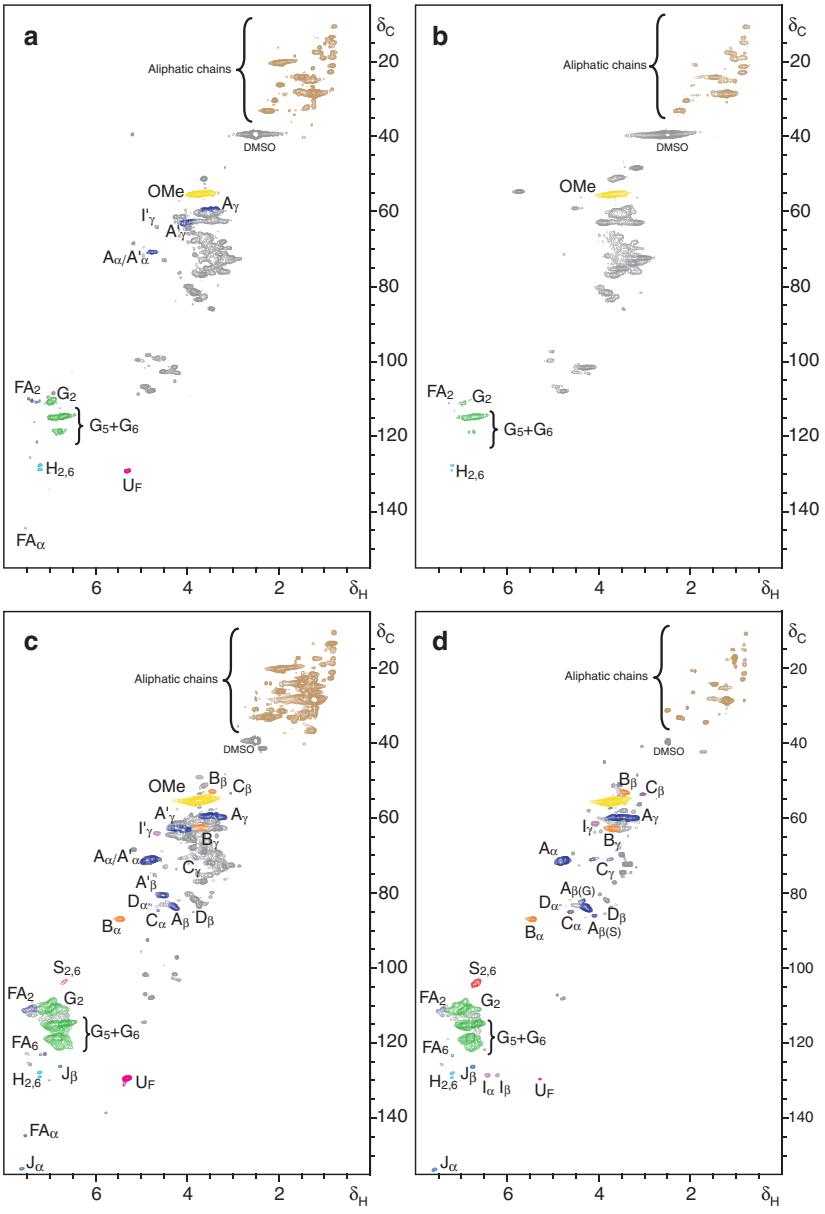

Figure 3: 2D-HSQC NMR spectra of *Quercus suber* cork and milled-cork lignin samples. (a) Extracted cork (Cork); (b) $Cork_{sap}$; (c) MCL; (d) MCL_{sap}. See Table 3 for signal assignments and Figure 4 for the main lignin structures identified.

methoxy groups (δ_C/δ_H 55.6/3.73) and side-chains in β–*O*–4′-substructures (**A**) are the most prominent. The C_α–H_α correlations in β–*O*–4′-substructures are seen at δ_C/δ_H 70.9/4.71 and the C_β–H_β correlations are at δ_C/δ_H 83.4/4.27 in β–*O*–4′-substructures linked to a G-unit, whereas a small signal at δ_C/δ_H 85.8/4.11 is for β–*O*–4′-substructures linked to S-units. Other lignin substructures are more clearly visible in the HSQC spectra of the MCL samples, particularly in MCL_{sap}, including signals for phenylcoumarans (**B**) and resinols (**C**). The signals for the C_α–H_α and C_β–H_β correlations of phenylcoumaran (β–5′) substructures are at δ_C/δ_H 86.8/5.43 and 53.1/3.43, whereas their C_γ–H_γ correlation overlaps with other C_γ–H_γ signals around δ_C/δ_H 62.6/3.67. Small signals for resinol (β–β′) substructures are present in the spectra of MCL and MCL_{sap}, with their C_α–H_α, C_β–H_β and the double C_γ–H_γ correlations at δ_C/δ_H 84.8/4.65, 53.5/3.05 and 71.0/3.81, and 4.17, respectively. In addition, small signals for the C_α–H_α and C_β–H_β correlations of dibenzodioxocin (**D**) substructures are visible in the spectra of MCL and MCL_{sap} at δ_C/δ_H 83.3/4.81 and 85.3/3.85, respectively. Other signals in the side-chain region of the MCL_{sap} correspond to C_γ–H_γ correlations (at δ_C/δ_H 61.3/4.08) assigned to cinnamyl alcohol end-groups (**I**). Interestingly, the HSQC spectra of the non-saponified

Table 3: Assignments of the lignin ^{13}C–^{1}H correlation peaks in the 2D-NMR HSQC spectra of *Quercus suber* cork and derived samples.

Label	δ_C/δ_H (ppm)	Assignment
B_β	53.1/3.43	C_β–H_β in phenylcoumaran substructures (**B**)
C_β	53.5/3.05	C_β–H_β in β–β′ resinol substructures (**C**)
-OCH_3	55.6/3.73	C–H in methoxyls
A_γ	59.4/3.40 and 3.72	C_γ–H_γ in γ-hydroxylated β–*O*–4′ substructures (**A**)
I_γ	61.3/4.08	C_γ–H_γ in cinnamyl alcohol end-groups (**I**)
B_γ	62.6/3.67	C_γ–H_γ in phenylcoumaran substructures (**B**)
A'_γ	62.7/3.83–4.19	C_γ–H_γ in γ-acylated β–*O*–4′ substructures (**A′**)
I'_γ	64.0/4.79	C_γ–H_γ in γ-acylated cinnamyl alcohol end-groups (**I′**)
$A_{\alpha(G)}$	70.9/4.71	C_α–H_α in β–*O*–4′ substructures (**A**) linked to a G-unit
C_γ	71.0/3.81 and 4.17	C_γ–H_γ in β–β′ resinol substructures (**C**)
$A'_{\beta(G)}$	80.8/4.52	C_β–H_β in γ-acylated β–*O*–4′ substructures (**A′**) linked to a G-unit
D_α	83.3/4.81	C_α–H_α in 5–5′ dibenzodioxocin substructures (**D**)
$A_{\beta(G)}$	83.4/4.27	C_β–H_β in β–*O*–4′ substructures (**A**) linked to a G-unit
C_α	84.8/4.65	C_α–H_α in β–β′ resinol substructures (**C**)
D_β	85.3/3.85	C_β–H_β in 5–5′ dibenzodioxocin substructures (**D**)
$A_{\beta(S)}$	85.8/4.11	C_β–H_β in β–*O*–4′ substructures (**A**) linked to a S-unit
B_α	86.8/5.43	C_α–H_α in phenylcoumaran substructures (**B**)
$S_{2,6}$	103.8/6.69	C_2–H_2 and C_6–H_6 in etherified syringyl units (**S**)
G_2	110.9/6.99	C_2–H_2 in guaiacyl units (**G**)
FA_2	111.0/7.32	C_2–H_2 in ferulates (**FA**)
G_5/G_6	114.9/6.72 and 6.94, and 118.7/6.77	C_5–H_5 and C_6–H_6 in guaiacyl units (**G**)
J_β	126.3/6.76	C_β–H_β in cinnamyl aldehyde end-groups (**J**)
$H_{2,6}$	127.8/7.22	$C_{2,6}$–$H_{2,6}$ in *p*-hydroxyphenyl units (**H**)
I_β	128.4/6.23	C_β–H_β in cinnamyl alcohol end-groups (**I**)
I_α	128.4/6.44	C_α–H_α in cinnamyl alcohol end-groups (**I**)
FA_α	144.7/7.41	C_α–H_α in ferulates (**FA**)
J_α	153.4/7.61	C_α–H_α in cinnamyl aldehyde end-groups (**J**)

samples (Cork and MCL) clearly show the presence of some signals of the partial acylation of lignin at the γ-carbon of the side-chain. The most characteristic signal is from the C_β–H_β correlations of γ-acylated β–*O*–4′-substructures (**A′**) linked to a G-unit that is clearly observed at δ_C/δ_H 80.8/4.52 in the spectrum of MCL, indicating an important acylation extent of a G-lignin. The signals of the C_γ–H_γ correlations of γ-acylated units (**A′**) are present within the range of δ_C/δ_H 62.7/3.83–4.19, although they are partially overlapped with some carbohydrate signals. Other characteristic signal in the side-chain region indicative of γ-acylation corresponds to C_γ–H_γ correlations (at δ_C/δ_H 64.0/4.79) of γ-acylated cinnamyl alcohol end-groups (**I′**), which are clearly visible in the spectra of Cork and MCL. Acylation at the α-carbon can be ruled out because of the absence of the corresponding signals in the HSQC spectra. An estimation of the percentage of γ-acylation was performed by integrating the signals corresponding to the hydroxylated (**A**) vs. acylated (**A′**) C_β–H_β correlations in the HSQC spectra of MCL, where the signals are better resolved and carbohydrates do not interfere, and accounted for about 50%. The signals indicating acylation of the γ-carbon were not observed in $Cork_{sap}$ and MCL_{sap} because of the hydrolysis of the ester groups. In summary, the HSQC data indicate that lignin in cork is heavily acylated exclusively at the γ-position, although it cannot provide additional information on the nature of the acylating group and therefore additional experiments would be needed to definitively asses the structure of the acylating group. However, strong signals for acetate groups were also observed in the HSQC spectra of Cork and MCL at δ_C/δ_H 20.3/1.90, indicating that acetates might be the acylating group on the γ-OH of this lignin, which is common in the case of other lignins (del Río et al. 2007b, 2008, 2012). In most plants, acetylation of the lignin on γ-OH occurs predominantly on S-units, and sinapyl acetate has been demonstrated to be a lignin monomer participating in coupling and cross-coupling reaction during lignification (Lu and Ralph 2002, 2008; del Río et al. 2007b, 2008). Thus, it can be assumed that coniferyl acetate could also act as a monomer in *Q. suber* cork participating in lignification and implicates the activity of corresponding acetyl transferases in *Q. suber* cork.

The main cross-signals in the aromatic regions of the HSQC spectra correspond to the different lignin units and

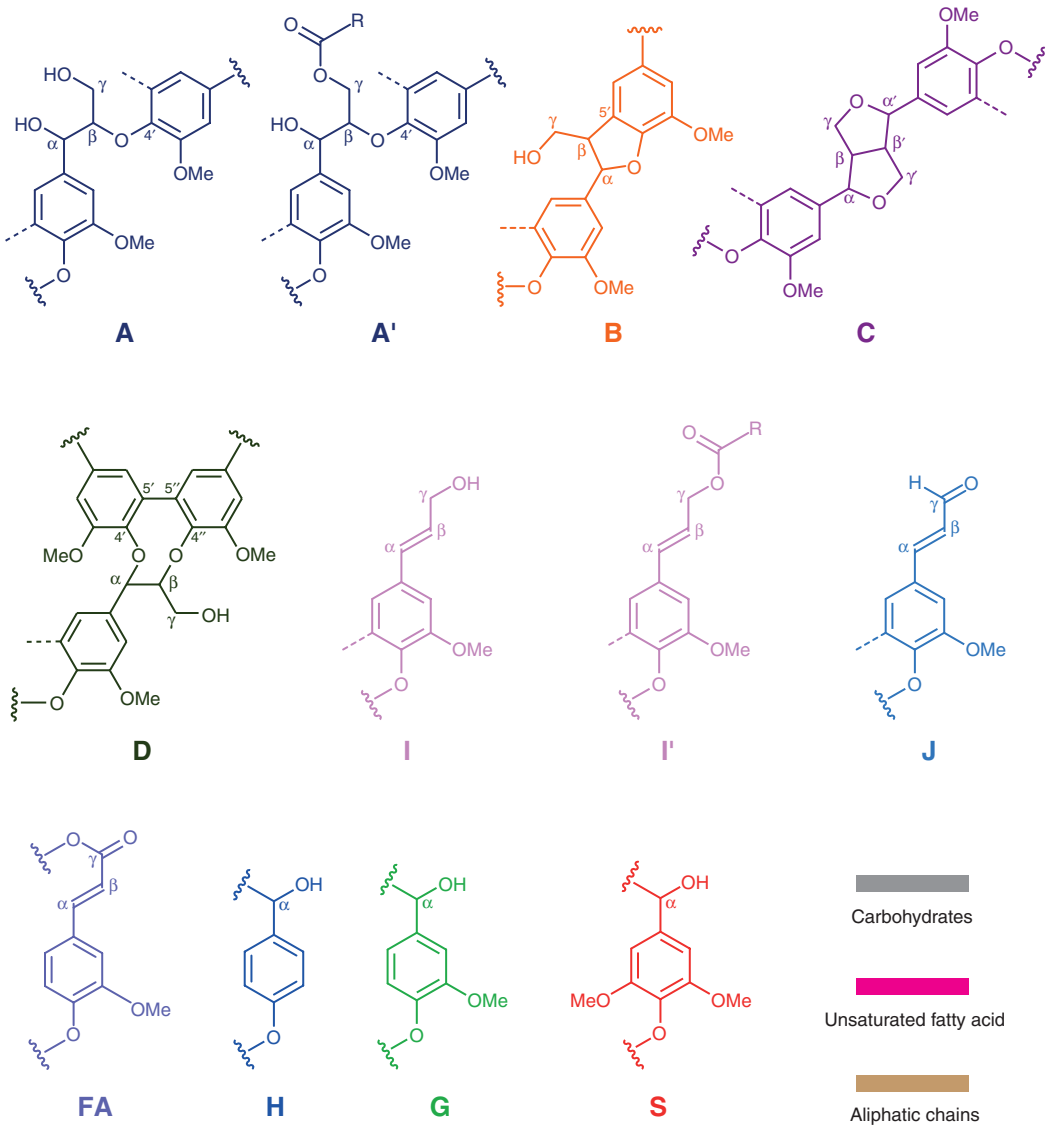

Figure 4: Main structures present in *Quercus suber* cork and milled-cork lignin samples: (**A**) β–*O*–4′ alkyl-aryl ethers; (**A′**) γ-acylated β–*O*–4′ alkyl-aryl ethers; (**B**) phenylcoumarans; (**C**) resinols; (**D**) dibenzodioxocins; (**I**) cinnamyl alcohol end-groups; (**I′**) γ-acylated cinnamyl alcohol end-groups; (**J**) cinnamyl aldehyde end-groups; (**FA**) ferulates; (**H**) *p*-hydroxyphenyl units; (**G**) guaiacyl units; (**S**) syringyl units.

to ferulates. Signals from G units, and to a lower extent, from H and S units, are present in the $Cork_{sap}$ and MCL and MCL_{sap} samples. The G units show different correlations for C_2–H_2 (δ_C/δ_H 110.9/6.99), and for C_5–H_5 and C_6–H_6 (δ_C/δ_H 114.9/6.72 and 6.94, and 118.7/6.77, respectively). The S units, observed mostly in MCL_{sap}, show a signal for the $C_{2,6}$–$H_{2,6}$ correlation at δ_C/δ_H 103.8/6.69, whereas the signals for $C_{2,6}$–$H_{2,6}$ of H units at δ_C/δ_H 127.8/7.22 are also detectable, although in low amounts. Signals corresponding to the C_2–H_2 correlations of ferulates were observed at δ_C/δ_H 111.0/7.32 in all the spectra, together with small signals for the correlations corresponding to the unsaturated C_α–H_α at δ_C/δ_H 144.7/7.41 in the spectra of Cork and MCL. In this region, a signal around δ_C/δ_H 127.9/7.36 is visible, although at a low intensity (not shown in the HSQC spectra of Figure 3), which is a characteristic of the C_7–H_7 correlation of the 8–*O*–4′-coupled dimeric product of ferulates (Ralph et al. 1994). This signal was only observed in the case of MCL and MCL_{sap}, and its presence is an indication that ferulates are involved in coupling reactions and participate in the lignification of cork. This finding is in agreement with the previously reported identification of FA dimers in cork (Graça 2010). Other signals in this HSQC region of the spectra are from unsaturated carbons of cinnamyl alcohol end-groups (**I**), with their C_α–H_α and C_β–H_β correlations observed at δ_C/δ_H 128.4/6.44 and 128.4/6.23, and cinnamaldehyde end-groups (**J**), with the C_α–H_α and C_β–H_β correlations observed at δ_C/δ_H 153.4/7.61 and 126.3/6.76,

respectively. The total relative content of the cinnamaldehyde end-groups were estimated by comparison of the intensities of the C_β–H_β correlations in cinnamyl alcohols (**I**) and aldehydes (**J**).

The relative abundances of the main lignin inter-unit linkages, end-groups, percentage of γ-acylation, aromatic units, S/G ratio and ferulate content estimated from volume integration of contours in the HSQC spectra of *Q. suber* cork and derived samples, are shown in Table 4. The data indicate that the structure of MCL and MCL_{sap} is mostly made up of β–*O*–4′ linkages (accounting for 80% and 77% of all inter-unit linkages, respectively) followed by phenylcoumarans (18% and 20% in MCL and MCL_{sap}, respectively), with lower amounts of resinols (ca. 2%) and dibenzodioxocins (1%). Cinnamyl end-groups (**I**, **J**) are present in relatively high abundances. In MCL, cinnamyl alcohol end-groups are mostly γ-acylated (9%) with only small amounts (1%) of normal γ-OH cinnamyl alcohol end-groups (**I**), whereas cinnamyl alcohol end-groups in MCL_{sap} are free. Accordingly, the major part of the cinnamyl alcohol-end groups are esterified in the cork (its γ-OH is acylated), which are then cleaved after alkaline transesterification. The same occurs with the other lignin substructures, such as the β–*O*–4′ alkyl-aryl ethers, which are partially acylated at the γ-OH in the MCL, but are completely hydrolyzed after alkaline transesterification and are absent in MCL_{sap}.

The NMR results in terms of H/G/S ratios match roughly to that by Py-TMAH, and confirm the preponderance of G units (up to 98% in MCL). The 2D-NMR profile fulfils all the characteristics of a G-lignin as previously reported for MCL_{sap}. The ferulates content also roughly matches those obtained upon Py-TMAH. However, and in contrast to Py-TMAH observations, only residual amounts of suberin aliphatic acids and carbohydrates are still visible in the HSQC spectra of MCL_{sap}, which may represent moieties intimately linked to lignin. The relatively high proportions of H units found by HSQC in Cork and $Cork_{sap}$ (8–9% of total lignin units), with respect to those present in their respective MCL and MCL_{sap} samples (1%), and to those found by Py-TMAH, may indicate the presence of proteins in these materials that give a signal similar to the H units.

Role of ferulates in the assembly of cork matrix

Lignin in *Q. suber* cork amounts to 22%, which is approximately half of the suberin content (Pereira 2013). Lignin is present in the middle lamella and is part of the secondary wall of the cork cells, acting as a supporting framework of the CW (Pereira and Marques 1988). The results of the present study indicate that FA is roughly equally distributed among the lignin and suberin moieties. In fact, FA is assembled into the cork matrix by two types of linkages: 1) ester/ether linkages that are alkaline labile and release FA molecules upon suberin depolymerisation (Table 1) – the FA in this situation represent about 1.6% of cork (2.7%

Table 4: Structural characteristics (lignin inter-unit linkages, end-groups, aromatic units and ferulate content) from integration of ^{13}C–^{1}H correlation peaks in the HSQC spectra of *Quercus suber* cork and derived samples.

	Cork	$Cork_{sap}$	MCL	MCL_{sap}
Lignin inter-unit linkages (%)				
β–*O*–4′ alkyl-aryl ethers (**A**/**A′**)	–	–	80	77
β–5′ phenylcoumarans (**B**)	–	–	18	20
β–β′ resinols s (**C**)	–	–	1	2
5–5′ dibenzodioxocins (**D**)	–	–	1	1
Lignin end-groups[a]				
Cinnamyl alcohol end-groups (**I**)	–	–	1	10
γ-acylated cinnamyl alcohol end-groups (**I′**)	–	–	9	0
Cinnamaldehyde end-groups (**J**)	–	–	7	6
Percentage of γ-acylation	–	–	50	0
Lignin aromatic units[b]				
H (%)	8	9	1	1
G (%)	92	91	98	96
S (%)	0	0	1	3
Ferulates[c]	8	3	8	6

[a]Expressed as a fraction of the total lignin inter-unit linkage types **A–C**.
[b]Molar percentages (H+G+S=100).
[c]Ferulate levels expressed as a fraction of lignin content (H+G+S).

in the suberin extract, which accounts for 58.5% of the cork); and 2) ether linkages that are alkaline resistant and remain in the solid residue after suberin removal ($Cork_{sap}$, Table 2) –this FA represent about 1.4% of cork (3.3% in the $Cork_{sap}$, which accounts for 41.5% of the cork).

It can be concluded that the lignin domain contains twice as much FA than the suberin domain. Ferulates are not responsible for the observed lamellation in cork CW and are not necessarily required for the suberin macroaliphatic construction (Serra et al. 2010a). It can be speculated that ferulates play a cross-linking role between the cork structural-macro moieties, although there is no chemical evidence hitherto to this assumption.

Incorporation of ether-bonded FA in the lignin matrix allows for the establishment of ester bonds of the macromolecule with hydroxyl groups of other chemical entities, such as ω-hydroxyacids from suberins or carbohydrates, thereby strengthening the CW framework. This cross-linking role has already been established for non-woody plants (Hatfield et al. 1999), and ferulates of ω-hydroxyacids and diferulates have been identified in suberin depolymerizates (Graça 2010). The presence of residual amounts of suberin aliphatics and carbohydrates in MCL_{sap} might also indicate the existence of alkaline-resistant bonds between these moieties.

In other suberized tissues, the content of ferulates may be much higher than the values observed in the present study, thereby resulting in a lignin matrix differing from the conventional lignin composition. In fact, Bernards et al. (1995) identified in wound-healing suberized potato tissues a polyphenolic moiety, which was characterized as a covalently linked hydroxycinnamate-derived polymer matrix, with only minute amounts of lignin.

Conclusion

Py-TMAH and 2D-HSQC-NMR analyses demonstrated that cork lignin is essentially a G-lignin with more than 96% G units, the structure of which is largely dominated by β–*O*–4′ alkyl-aryl ether linkages (80% and 77% in MCL and MCL_{sap}, respectively), followed by phenylcoumarans (18% and 20% in MCL and MCL_{sap}, respectively), and smaller amounts of resinols (ca. 2%) and dibenzodioxocins (1%). The lignin in cork is heavily acylated (up to 50%) at the γ-OH of the side-chain. Ferulates are part of the lignin structure, where it represent about 6% of the lignin, and seem to be involved in linkages between lignin and suberin. Overall, FA represents up to 3% of the cork and is incorporated into the suberin and lignin structures, where it seems to have an important function in the chemical assembly of cork CWs with a cross-linking role between the structural macromolecules of suberin, lignin, and carbohydrates. FA contributes to the properties of cork tissues along with compositional variations and other possible suberin-lignin linkages.

Acknowledgments: We acknowledge partial financial support from Instituto Politécnico de Lisboa, Portugal (Research Project IPL 19/2003) and base funding from Fundação para a Ciência e Tecnologia, Portugal (FCT research Unit 702) to Centro de Estudos Florestais (PEstOE/AGR/UI0239/2014). This study was also partially funded by the LIGNOCELL project (AGL2011-25379) from the Spanish MICINN (co-financed by FEDER funds). JR acknowledges the CSIC JAE-Doc contract of the program "Junta para la Ampliaciôn de Estudios" co-financed by the European Social Fund (ESF). We also thank Dr. Manuel Angulo (CITIUS, University of Seville) for performing the NMR analyses.

References

Bento, M.F., Pereira, H., Cunha, M.A., Moutinho, A.M.C., van den Berg, K.J, Boon, J.J. (1998) Thermally assisted transmethylation gas chromatography-mass spectrometry of suberin components in cork from *Quercus suber* L. Phytochem. Anal. 9:75–87.

Bento, M.F.S., Pereira, H., Cunha, M.A., Moutinho, A.M.C., van den Berg, K.J., Boon, J.J. (2001) A study of variability of suberin composition in cork from *Quercus suber* L. using thermally assisted transmethylation GC–MS. J. Anal. Appl. Pyrol. 57:45–55.

Bernards, M.A. (2002) Demystifying suberin. Can. J. Bot. 240:227–240.

Bernards, M.A., Lopez, M.L., Zajicek, J., Lewis, N.G. (1995) Hydroxycinnamic acid-derived polymers constitute the polyaromatic domain of suberin. J. Biol. Chem. 270:7382–7386.

Boher, P., Serra, O., Soler, M., Molinas, M., Figueras, M. (2013) The potato suberin feruloyl transferase FHT which accumulates in the phellogen is induced by wounding and regulated by abscisic and salicylic acids. J. Exp. Bot. 64:3225–3236.

Bonawitz, N.D., Chapple, C. (2010) The genetics of lignin biosynthesis: connecting genotype to phenotype. Annu. Rev. Genet. 44:337–436.

de Leeuw, J.W., Baas, M. (1993) The behaviour of esters in the presence of tetramethylammonium salts at elevated temperatures; flash pyrolysis or flash chemolysis? J. Anal. Appl. Pyrol. 26:175–184.

del Río, J.C., Martín, F., González-Vila, F.J. (1996) Thermally assisted hydrolysis and alkylation as a novel pyrolytic approach for the structural characterization of natural biopolymers and geomacromolecules. Trends Anal. Chem. 15:70–79.

del Río, J.C., Hatcher, P.G. (1998) Analysis of aliphatic biopolymers using thermochemolysis with tetramethylammonium hydroxide (TMAH) and gas chromatography-mass spectrometry. Org. Geochem. 29:1441–1451.

del Río, J.C., McKinney, D.E., Knicker, H., Nanny, M.A., Minard, R.D., Hatcher, P.G. (1998) Structural characterization of bio- and geomacromolecules by off-line thermochemolysis with tetramethylammonium hydroxide. J. Chromatogr. A 823:433–448.

del Río, J.C., Gutiérrez, A., Rodríguez, I.M., Ibarra, D., Martínez, Á.T. (2007a) Composition of non-woody plant lignins and cinnamic acids by Py-GC/MS, Py/TMAH and FT-IR. J. Anal. Appl. Pyrol. 79:39–46.

del Río, J.C., Marques, G., Rencoret, J., Martínez, A.T., Gutiérrez, A. (2007b) Occurrence of naturally acetylated lignin units. J. Agric. Food Chem. 55:5461–5468.

del Río, J.C., Rencoret, J., Marques, G., Gutiérrez, A., Ibarra, D., Santos, J.I., Jiménez-Barbero, J., Zhang, L., Martínez, A.T. (2008) Highly acylated (acetylated and/or *p*-coumaroylated) native lignins from diverse herbaceous plants. J. Agric. Food Chem. 56:9525–9534.

del Río, J.C., Rencoret, J., Gutiérrez, A., Nieto, L., Jiménez-Barbero, J., Martínez, Á.T. (2011) Structural characterization of guaiacyl-rich lignins in flax (*Linum usitatissimum*) fibers and shives. J. Agric. Food Chem. 59:11088–11099.

del Río, J.C., Rencoret, J., Prinsen, P., Martínez, Á.T., Ralph, J., Gutiérrez, A. (2012) Structural characterization of wheat straw lignin as revealed by analytical pyrolysis, 2D-NMR, and reductive cleavage methods. J. Agric. Food Chem. 60:5922–5935.

García-Vallejo, M.C., Conde, E., Cadahía, E., de Simón, B.F. (1997) Suberin composition of reproduction cork from *Quercus suber*. Holzforschung 51:219–224.

Gou, J.-Y., Yu, X.-H., Liu, C.-J. (2009) A hydroxycinnamoyltransferase responsible for synthesizing suberin aromatics in *Arabidopsis*. Proc. Natl. Acad. Sci. USA 106:18855–18860.

Graça, J. (2010) Hydroxycinnamates in suberin formation. Phytochem. Rev. 9:85–91.

Graça, J., Pereira, H. (1997) Cork suberin: a glyceryl based polyester. Holzforschung 51:225–234.

Graça, J., Pereira, H. (1998) Feruloyl esters of ω-hydroxyacids in cork suberin. J. Wood Chem. Technol. 18:207–217.

Graça, J., Pereira, H. (2000a) Suberin structure in potato periderm: glycerol, long-chain monomers, and glyceryl and feruloyl dimers. J. Agric. Food Chem. 48:5476–5483.

Graça, J., Pereira, H. (2000b) Methanolysis of bark suberins: analysis of glycerol and acid monomers. Phytochem. Anal. 11:45–51.

Hatfield, R.D., Ralph, J., Grabber, J.H. (1999) Cell wall cross-linking by ferulates and diferulates in grasses. J. Sci. Food Agric. 79:403–407.

Iglesias, G., Bao, M., Lamas, J., Vega, A. (1996) Soda pulping of *Miscanthus sinensis*. Effects of operational variables on pulp yield and lignin solubilization. Bioresour. Technol. 58:17–23.

Kolattukudy, P.E. (2001) Polyesters in higher plants. Adv. Biochem. Eng. Biotechnol. 71:1–49.

Kumar, L, Pruthi, V. (2014) Potential applications of ferulic acid from natural sources. Biotech. Reports 4:86–93.

Lapierre, C., Pollet, B., Négrel, J. (1996) The phenolic domain of potato suberin: structural comparison with lignins. Phytochemistry 42:949–953.

Lu, F., Ralph, J. (2002) Preliminary evidence for sinapyl acetate as a lignin monomer in kenaf. Chem. Commun. 1:90–91.

Lu, F., Ralph, J. (2008) Novel tetrahydrofuran structures derived from β–β-coupling reactions involving sinapyl acetates in kenaf lignins. Org. Biomol. Chem. 6:3681–3694.

Marques, A.V., Pereira, H. (2013) Lignin monomeric composition of corks from the barks of *Betula pendula*, *Quercus suber* and *Quercus cerris* determined by Py-GC-MS/FID. J. Anal. Appl. Pyrol. 100:88–94.

Marques, A.V., Pereira, H. (2014) Aliphatic bio-oils from corks: a Py-GC/MS study. J. Anal. Appl. Pyrol. 109:29–40.

Marques, A.V., Pereira, H., Meier, D., Faix, O. (1994) Quantitative analysis of cork (*Quercus Suber* L.) and milled cork lignin by FTIR spectroscopy, analytical pyrolysis, and total hydrolysis. Holzforschung 48:43–50.

Marques, A.V., Pereira, H., Meier, D., Faix, O. (1996) Isolation and characterization of a guaiacyl lignin from saponified cork of *Quercus suber* L. Holzforschung 50:393–400.

Marques, A.V., Pereira, H., Meier, D., Faix, O. (1999) Structural characterization of cork lignin by thioacidolysis and permanganate oxidation. Holzforschung 53:167–174.

Marques, A.V., Pereira, H., Rodrigues, J., Meier, D., Faix, O. (2006) Isolation and comparative characterization of a Björkman lignin from the saponified cork of Douglas-fir bark. J. Anal. Appl. Pyrol. 77:169–176.

Martín, F., del Río, J.C., González-Vila, Verdejo, T. (1995) Thermally assisted hydrolysis and alkylation of lignins in the presence of tetra-alkylammonium hydroxides. J. Anal. Appl. Pyrol. 35:1–13.

Miranda, I., Gominho, J., Pereira, H. (2013) Cellular structure and chemical composition of cork from the Chinese cork oak (*Quercus variabilis*). J. Wood Sci. 59:1–9.

Molina, I., Li-Beisson, Y., Beisson, F., Ohlrogge, J.B., Pollard, M. (2009) Identification of an *Arabidopsis* feruloyl-coenzyme A transferase required for suberin synthesis. Plant Physiol. 151:1317–1328.

Olivella, M.A., del Río, J.C. (2011) Suberin composition from different bark layers of *Quercus suber* L. by Py-GC/MS in the presence of tetramethylammonium Hydroxide (TMAH). BioResources 6:4936–4941.

Pereira, H. Cork: Biology, Production and Uses. Elsevier, Amesterdam, 2007.

Pereira, H. (2013) Variability of the chemical composition of cork. BioResources 8:2246–2256.

Pereira, H., Marques, A.V. (1988) The effect of chemical treatments on the cellular structure of cork. IAWA Bull. 9:337–345.

Pinto, P.C.R.O., Sousa, A.F., Silvestre, A.J.D., Neto, C.P., Gandini, A., Eckerman, C., Holmbom, B. (2009) *Quercus suber* and *Betula pendula* outer barks as renewable sources of oleochemicals: a comparative study. Ind. Crops Prod. 29:126–132.

Ralph, J. (2010) Hydroxycinnamates in lignification. Phytochem. Rev. 9:65–83.

Ralph, J., Quideau, S., Grabber, J.H., Hatfield, R.D. (1994) Identification and synthesis of new ferulic acid dehydrodimers present in grass cell-walls. J. Chem. Soc. Perkin Trans. 1:3485–3498.

Ralph, J., Bunzel, M., Marita, J., Hatfield, R., Lu, F., Kim, H., Schatz, P.F., Grabber, J.H., Steinhart, H. (2004a) Peroxidase-dependent cross-linking reactions of *p*-hydroxycinnamates in plant cell walls. Phytochem. Rev. 3:79–96.

Ralph, J., Lundquist, K., Brunow, G., Lu, F., Kim, H., Schatz, P.F., Marita, J.M., Hatfield, R.D., Ralph, S.A., Christensen, J.H., Boerjan, W. (2004b) Lignins: natural polymers from oxidative coupling of 4-hydroxyphenyl-propanoids. Phytochem. Rev. 3:29–60.

Ralph, S., Landucci, L., Ralph, J. (2004c) NMR Database of Lignin and Cell Wall Model Compounds [WWW Document]. US For.

Prod. Lab., One Gifford Pinchot Dr., Madison, WI 53705, Accessed January 2009.

Rencoret, J., Marques, G., Gutiérrez, A., Ibarra, D., Li, J., Gellerstedt, G., Santos, J.I., Jiménez-Barbero, J., Martínez, Á.T., del Río, J.C. (2008) Structural characterization of milled wood lignins from different eucalypt species. Holzforschung 62:514–526.

Rencoret, J., Marques, G., Gutiérrez, A., Nieto, L., Jiménez-Barbero, J., Martínez, Á.T., del Río, J.C. (2009) Isolation and structural characterization of the milled-wood lignin from *Paulownia fortunei* wood. Ind. Crops Prod. 30:137–143.

Rencoret, J., Gutiérrez, A., Nieto, L., Jiménez-Barbero, J., Faulds, C.B., Kim, H., Ralph, J., Martínez, A.T., del Río, J.C. (2011) Lignin composition and structure in young versus adult *Eucalyptus globulus* plants. Plant Physiol. 155:667–682.

Santos, S., Graça, J. (2006) Glycerol-ω-hydroxyacid-ferulic acid oligomers in cork suberin structure. Holzforschung 60:171–177.

Scalbert, A., Monties, B., Rolando, C., Sierra-Escudero, A. (1986) Formation of ether linkage between phenolic acids and gramineae lignin: a possible mechanism involving quinone methides. Holzforschung 40:191–195.

Sederoff, R.R., MacKay, J.J., Ralph, J., Hatfield, R.D. (1999) Unexpected variation in lignin. Curr. Opin. Plant Biol. 2:145–52.

Şen, A., Miranda, I., Santos, S., Graça, J., Pereira, H. (2010) The chemical composition of cork and phloem in the rhytidome of *Quercus cerris* bark. Ind. Crops Prod. 31:417–422.

Serra, O., Soler, M., Hohn, C., Sauveplane, V., Pinot, F., Franke, R., Schreiber, L., Prat, S., Molinas, M., Figueras, M. (2009) CYP86A33-targeted gene silencing in potato tuber alters suberin composition, distorts suberin lamellae, and impairs the periderm's water barrier function. Plant Physiol. 149: 1050–60.

Serra, O., Figueras, M., Franke, R., Prat, S., Molinas, M. (2010a) Unraveling ferulate role in suberin and periderm biology by reverse genetics. Plant Signal. Behav. 5:953–958.

Serra, O., Hohn, C., Franke, R., Prat, S., Molinas, M., Figueras, M. (2010b) A feruloyl transferase involved in the biosynthesis of suberin and suberin-associated wax is required for maturation and sealing properties of potato periderm. Plant J. 62: 277–290.

Soler, M., Serra, O., Molinas, M., Huguet, G., Fluch, S., Figueras, M. (2007) A genomic approach to suberin biosynthesis and cork differentiation. Plant Physiol. 144:419–431.

Tegelaar, E.W., Hollman, G., Van Der Vegt, P., De Leew, J.W., Holloway, P.J. (1995) Chemical characterization of the periderm tissue of some angiosperm species: recognition of an insoluble, non-hydrolyzable, aliphatic biomacromolecule (suberan). Org. Geochem. 23:239–250.

Turner, J.W., Hartman, B.E., Hatcher, P.G. (2013) Structural characterization of suberan isolated from river birch (*Betula nigra*) bark. Org. Geochem. 57:41–53.

Vanholme, R., Demedts, B., Morreel, K., Ralph, J., Boerjan, W. (2010) Lignin biosynthesis and structure. Plant Physiol. 153:895–905.

Yan, B., Stark, R.E. (2000) Biosynthesis, molecular structure, and domain architecture of potato suberin: a 13C NMR study using isotopically labeled precursors. J. Agric. Food Chem. 48:3298–3304.